bioRxiv preprint doi: https://doi.org/10.1101/324368; this version posted May 16, 2018. The copyright holder for this preprint (which was not certified by peer review) is the author/funder, who has granted bioRxiv a license to display the preprint in perpetuity. It is made available under aCC-BY 4.0 International license.

Rampant cryptic sex chromosome drive in Drosophila

Chris Ellison[1], Chris Leonard[2], Emily Landeen[1], Lauren Gibilisco[1], Nitin Phadnis[2] and Doris Bachtrog[1]

[1]*University of California Berkeley, Berkeley, CA 94720*

[2]*University of Utah, Salt Lake City, UT 84112*

*corresponding author: dbachtrog@berkeley.edu

Theory predicts that selfish genetic elements that increase their transmission are prone to originate on sex-chromosomes but create strong selective pressure to evolve suppressors due to reduced fertility and distorted population sex-ratios. Here we show that recurrent genetic conflict over sex-chromosome transmission is an important evolutionary force that has shaped gene-content evolution of sex-chromosomes. We demonstrate that convergent acquisition and amplification of spermatid-expressed gene-families are common on Drosophila sex-chromosomes, and harbor characteristics typical of meiotic drivers. We experimentally verify a novel cryptic sex-chromosome-distortion system in *Drosophila pseudoobscura* using transgenics. Knockdown of Y-linked copies of the *S-Lap1* gene-family result in abnormal spermatogenesis, a deficiency of Y-bearing sperm and female-biased sex-ratios, and meiotic drive and suppression likely involves RNAi mechanisms. Our finding suggests that recurrent conflict over sex-chromosome transmission has shaped widespread genomic and evolutionary patterns, including the epigenetic regulation of sex-chromosomes, the distribution of sex-biased-genes, and the evolution of hybrid sterility.

Segregation distorters (also known as meiotic drivers) are selfish genetic elements that manipulate meiosis or gametogenesis to increase their own transmission (Sandler and Novitski 1957). All characterized meiotic drive systems involve a distorting locus that targets a sensitive responder locus on its homolog, so that the chromosome where the driver resides is transmitted to more than 50% of the offspring of a heterozygous carrier (Meiklejohn and Tao 2010). A distorter must be able to discriminate its host chromosome from its homolog, and the distorter and responder loci must be in strong linkage to avoid the generation of suicide chromosomes that carry the distorter and a sensitive responder (Jaenike 2003); both of these conditions are met on differentiated, non-recombining X and Y chromosomes. Thus, while segregation distorters can arise on all chromosomes, they are particularly prone to evolve on sex chromosomes (Jaenike 2003). Segregation distorters give rise to genetic conflicts among loci linked to the sensitive responder allele, and thus favor the evolution of loci that suppress distortion (Hurst and Werren 2001; Jaenike 2003). Disruption of equal transmission of the X and Y chromosomes, however, has the additional consequence of distorting population sex ratios and thus create strong selective pressure to evolve loci that repress sex ratio drive (Hurst and Werren 2001; Lindholm *et al.* 2016).

bioRxiv preprint doi: https://doi.org/10.1101/324368; this version posted May 16, 2018. The copyright holder for this preprint (which was not certified by peer review) is the author/funder, who has granted bioRxiv a license to display the preprint in perpetuity. It is made available under aCC-BY 4.0 International license.

Sex chromosome drive may thus be prevalent in evolution but is often cryptic, since bursts of meiotic drive elements arising on sex chromosomes should be followed by the quick invasion of suppressor alleles that restore equal sex ratios (Jaenike 2003; Lindholm *et al.* 2016). Cryptic drive systems are typically only revealed through detailed genetic manipulations or crosses between populations or species, but may leave common footprints at patterns of genome evolution. In particular, molecular characterization of meiotic drive systems in both mammals and fruit flies has revealed the following commonalities: In several cases, both the distorter and suppressor alleles are amplified on the X and Y chromosome (Balakireva *et al.* 1992; Cocquet *et al.* 2009; Soh *et al.* 2014). Suppressors were found to share common sequences with the distorter itself (Tao *et al.* 2007a; b) (Cocquet *et al.* 2009; 2012), and suppression is likely mediated by sequence homology through RNAi mechanisms (Tao *et al.* 2007a; b). Thus, cryptic sex chromosome drive has repeatedly led to characteristic patterns of gene amplification of homologous genes on both the X and the Y chromosomes that are targeted by short RNAs.

Here, we use bioinformatics and experimental analyses to assess the importance of sex chromosome drive across Drosophila species. To analyze gene content evolution and identify amplified X- and Y-linked genes, we sequenced both male and female genomic DNA in 26 Drosophila species from across the Drosophila phylogeny (**Table S1**). Roughly half of the species considered (11 out of 26) harbor the typical sex chromosome complement of Drosophila (that is, a single pair of ancient sex chromosomes, shared by all members of Drosophila). In addition to the ancestral pair of sex chromosomes, the other 15 species have a younger pair of “neo-sex” chromosomes, which formed when an autosome became fused to one or both of the ancient X and Y chromosomes (**Figure S1**). These younger “neo-sex” chromosomes are at various stages of evolving the typical properties of ancestral sex chromosomes, with neo-Y chromosomes losing their original genes and acquiring a genetically inert heterochromatic appearance, and neo-X chromosomes acquiring their unique gene content and sex-specific expression patterns (Lucchesi 1978; Bachtrog 2013). We identified putative Y-amplified genes based on male and female gene coverage without relying on a genome assembly (see Methods) and validated our approach using a high-quality genome assembly from *D. pseudoobscura* (**Figure S2**). Using this approach, we found 46 amplified Y-linked genes with co-amplified X homologs in 10 species (**Table 1, Table S2**). Interestingly, we find that the observed gene amplifications are more common in species with recently added neo-sex chromosomes (i.e. 9 out of 10 species have neo-sex chromosomes). Young sex chromosomes have many more genes that can evolve to cheat meiosis, and in the vast majority of cases the amplified genes were ancestrally present on the chromosome that formed the neo-sex chromosomes (**Table 1**). Also, young sex chromosomes may not yet be transcriptionally down-regulated during spermatogenesis, and sex-linked drivers may thus be less likely to be silenced (Meiklejohn and Tao 2010).

bioRxiv preprint doi: https://doi.org/10.1101/324368; this version posted May 16, 2018. The copyright holder for this preprint (which was not certified by peer review) is the author/funder, who has granted bioRxiv a license to display the preprint in perpetuity. It is made available under aCC-BY 4.0 International license.

Several features of these genes are typical of meiotic drive systems identified in flies and mammals. First, consistent with their proposed action of cheating fair meiosis, many are highly expressed in reproductive tissues in *D. melanogaster* (**Table S2**), and several of the genes have meiosis-related functions that may be exploited for sex chromosome drive (**Table 1, Table S2**). For example, we identify genes that are associated with spindle assembly involved in male meiosis (*fest*), chromosome segregation (*mars*), or male meiosis cytokinesis (*scra*), amongst others (**Table 1**).

We decided to more carefully characterize a putative cryptic drive system in *D. pseudoobscura,* a species with a high quality PacBio-based genome assembly. *D. pseudoobscura* currently lacks an assembled Y chromosome, but we inferred Y-linkage of contigs based on male and female read coverage using Illumina data (see Methods). We identified two adjacent genes that exist in multiple copies on the X and Y chromosome of *D. pseudoobscura*: *S-Lap1* (Dpse\GA19547) and *GAPsec* (Dpse\GA28668). *S-Lap1* is a member of a leucyl aminopeptidase gene family that encodes the major protein constituents of Drosophila sperm (Dorus *et al.* 2011), while *GAPsec* is a GTPase activating protein. This situation is reminiscent of the *Segregation distorter* meiotic drive system in *D. melanogaster*, where the distorter is a tandem duplication of RanGAP, which is also a GTPase activator (Merrill 1999). Both *S-Lap1* and *GAPsec* show partial tandem duplications on the X (**Figure 1A**), and we detect roughly 100 (partial and full-length) copies of both *S-Lap1* and *GAPsec* on the Y chromosome (the Y-linked contigs contain 127 copies of *S-Lap1* and 91 copies of *GAPsec*; **Figure 1B, Figure S3**). *S-Lap1* appears to have independently duplicated in different parts of the Drosophila phylogeny (**Figure 1C**), while the partial duplication of *GAPsec* is only found in *D. pseudoobscura* and its close relative *D. persimilis* (**Figure 1C**). *S-Lap1* and *GAPsec* probably dispersed onto the Y chromosome simultaneously, as there are multiple locations on the Y that preserve their X orientation (**Figure 1B**); note however, that the amplified copies on the Y do not include the tandemly duplicated copies. For both *S-Lap1* and *GAPsec*, the X- and Y-linked copies are highly expressed in testis of *D. pseudoobscura* (**Table S2**), as expected for genes that try to cheat fair male meiosis.

To functionally verify whether *S-Lap1* is indeed involved in conflicts over sex chromosome transmission, we used RNA interference (RNAi) knockdown constructs that target only the Y-linked copies of *S-Lap1* but not the X-linked copies to deplete (knock down) the expression of the Y-linked duplicates of *S-Lap1* in *D. pseudoobscura* testes (**Figure 2A**). We produced transgenic *D. pseudoobscura* strains that carry this construct under the control of the testes-specific β-tubulin (Dpse\GA21728) promoter of *D. pseudoobscura* (**Figure S4**). RNA-seq experiments verified that our RNAi constructs down-regulated the expression of the Y-linked copies of *S-Lap1* relative to control flies (**Table S3**). Most interestingly, *D. pseudoobscura* males that carry this transgene produced progeny with highly female-biased sex ratios (~66 and 89% daughters in two independently derived transgenic lines; $P<0.01$, *t-test*, **Figure 2B, Figure S5**), while *white* control males produce equal sex ratios (**Figure 2B**). Embryonic

bioRxiv preprint doi: https://doi.org/10.1101/324368; this version posted May 16, 2018. The copyright holder for this preprint (which was not certified by peer review) is the author/funder, who has granted bioRxiv a license to display the preprint in perpetuity. It is made available under aCC-BY 4.0 International license.

survival rates were similar between transgenic lines and control males (**Table S4**), showing that biased sex ratios are not caused by male-specific lethality. Thus, knockdown of Y-linked copies of *S-Lap1* indeed reveals a cryptic sex chromosome drive system in *D. pseudoobscura*. To test whether males with reduced expression of the Y-linked copies of *S-Lap1* produce fewer Y-bearing sperm, we quantified the relative abundance of Y-containing sperm in RNAi knockdown vs. *white* control males. Specifically, we performed qPCR on genomic DNA from sperm isolated from seminal vesicles (**Figure S6**), and quantified abundance of a Y-linked locus vs. an autosomal reference gene in transgenic and control males. Indeed, we find a deficiency of Y-bearing sperm in RNAi lines ($P<0.01$, *t-test*; **Figure 2C**), suggesting that depletion of expression of Y-linked *S-Lap1* copies interferes with maturation of Y-containing sperm. Cytological examination of the testes of these transgenic males revealed developmental effects of spermatogenesis that are typical of meiotic drive (**Figure 3**) (Policansky and Ellison 1970). In particular, we observed an overall temporal delay in spermatogenesis, with many cysts failing to form competent sperm (**Figure 3A**). In bundles of more fully developed sperm, some nuclei fail to condense, leading to cysts with heterogeneous nuclear condensation, in contrast to wild-type spermatogenesis, where nuclear condensation is synchronous within each cyst (**Figure 3B**). Similar to the *Sex-Ratio* system of *D. pseudoobscura* (Policansky and Ellison 1970), developing cysts in the distorting background lack the full number of sperm in each cyst, as there are only about half as many sperm per cyst as compared to wildtype (**Figure 3C**). Together, these observations show that reducing expression of Y-linked *S-Lap1* genes results in meiotic drive through the elimination of Y-bearing sperm, and reveals that the Y-linked copies of *S-Lap1* are indeed involved in suppressing a cryptic X-linked driver.

In several cases, meiotic drive and suppression involves RNAi mechanisms. We gathered stranded RNA-seq and small RNA profiles from wildtype *D. pseudoobscura* testes, to obtain insights into the molecular mechanism of meiotic drive involving *S-Lap1*. Interestingly, we detect both sense and antisense transcripts and short RNA's derived from *S-Lap1* (**Figure 4A**). These data suggest a possible model of cryptic sex chromosome drive in *D. pseudoobscura*, where anti-sense production of *S-Lap1*-dup transcript may trigger siRNA production and silencing of *S-Lap1* (which is the most abundant sperm protein in *D. melanogaster* (Dorus *et al.* 2011)). This could result in elimination of Y-bearing sperm, and acquisition of multiple copies of S-*Lap1* on the Y chromosome could restore *S-Lap1* function, creating the cryptic drive system that we uncovered in *D. pseudoobscura* (**Figure 4B**). Detailed molecular testing will be necessary to characterize the wildtype function of *S-Lap1*, and the cellular basis of the drive phenotype and its suppression.

To conclude, our comparative analysis reveals that sex chromosome drive is common in Drosophila and we find evidence of cryptic sex ratio distortion systems across distantly related species. Most of these species harbor neo-sex chromosomes, suggesting that sex ratio distorters have repeatedly evolved to exploit genomic vulnerabilities

bioRxiv preprint doi: https://doi.org/10.1101/324368; this version posted May 16, 2018. The copyright holder for this preprint (which was not certified by peer review) is the author/funder, who has granted bioRxiv a license to display the preprint in perpetuity. It is made available under aCC-BY 4.0 International license.

associated with the formation of new sex chromosomes. Several putative drive genes have well-characterized functions in meiosis ensuring precise chromosome segregation, and selfish elements have recurrently succeeded to manipulate these normally tightly regulated cellular processes. The prevalence of cryptic sex ratio drive systems in insects and animals may account for several evolutionary and molecular phenomena (Meiklejohn and Tao 2010). Sex ratio distorters can fuel the rapid turn-over of sex determination mechanisms across species (Bachtrog *et al.* 2014), and the transcriptional inactivation of sex chromosomes during spermatogenesis may have evolved as a defense against meiotic drive elements. The recurrent fixation of cryptic drive systems on sex chromosomes might explain the prominent role of the X chromosome in the evolution of hybrid sterility in a wide range of species (Frank 1991; Hurst and Pomiankowski 1991; Presgraves 2010; McDermott and Noor 2010; Zhang *et al.* 2015), and contribute to genomic biases in the location of sex-biased genes or gene duplicates (Emerson *et al.* 2004; Vibranovski *et al.* 2009). Our data further suggest that the production of antisense transcripts and small RNAs may be a common feature of meiotic drive elements, and that the short RNA pathway has an important role not only in controlling genomic parasites such as transposable elements, but also selfish genetic elements that try to exploit highly regulated cellular proceeses such as chromosome segregation (Wen *et al.* 2015). Future characterization of this and other drive systems will provide a full picture of how distorting elements manipulate and cheat meiosis, what molecular pathways or developmental processes are particularly vulnerable, and how the genome has launched evolutionary responses to counter distortion**.**

Methods

Genome sequencing & assembly

Strains were acquired from the Drosophila Species Stock Center (UC San Diego) or the EHIME stock center (Ehime University, Japan) as indicated in **Table S1**. For each strain, DNA was extracted from a single male and a single female, using the Qiagen Gentra Puregene cell kit. The Illumina TruSeq Nano DNA library preparation kit was used to prepare 100 bp paired-end sequencing libraries for all species except *D. robusta*, *D. melanica*, and *D. willistoni*. For these species, the Illumina Nextera DNA library preparation kit was used to prepare 150 bp paired-end sequencing libraries. The genome assemblies produced for this study are noted in **Table S1**. Assemblies were produced from the female data: reads were error-corrected using BFC (Li 2015) and assembled using IDBA-UD (Peng *et al.* 2012) with default parameters.

Identification of X-A fusions

X chromosome/autosome fusions were identified in two steps (Vicoso and Bachtrog 2013). For each species, genomic scaffolds were assigned to Muller elements based on their gene content, inferred from the results of a translated BLAST search of *D. melanogaster* peptides to the assembly of interest. Scaffolds smaller than 5kb were excluded. Next, the male and female Illumina data were separately mapped to the female assembly using Bowtie2 (Langmead and Salzberg 2012) and excluding alignments with mapping quality less than 20. The coverage ratio (M/F) was calculated for each scaffold that was assigned to a Muller element. The distribution of coverage ratios for each Muller element (**Figure S1**) was then examined to determine if any of the ancestral autosomes had become X-linked.

bioRxiv preprint doi: https://doi.org/10.1101/324368; this version posted May 16, 2018. The copyright holder for this preprint (which was not certified by peer review) is the author/funder, who has granted bioRxiv a license to display the preprint in perpetuity. It is made available under aCC-BY 4.0 International license.

Identification of co-amplified genes on the X- and Y-chromosome

To characterize co-amplified genes on the sex chromosomes, we first identify genes amplified on the Y. For each species, male and female Illumina reads were separately aligned to a filtered version of the *D. melanogaster* peptide set, where only the longest isoform of each gene was retained. To generate these alignments, the DIAMOND software package (Buchfink *et al.* 2015) was used to perform a translated search of each Illumina read to the peptide set. Read coverage for each peptide sequence was calculated in 30 amino acid non-overlapping windows and normalized by dividing by the total number of mapped reads. The M/F coverage ratio was computed by dividing the median male coverage by the median female coverage, for each peptide. We required that potentially Y-amplified genes have a normalized M/F coverage ratio of at least 2.5 and only retained genes whose parent copy was X-linked in the species of interest. We searched for X-linked duplicates in the female genome assemblies by first using Exonerate (Slater and Birney 2005) to extract the coding sequence of the best hit between the *D. melanogaster* peptide and the female assembly. We then used BLASTN (Camacho *et al.* 2009) to obtain a stringent (E-value threshold = 1e-20) list of all non-overlapping hits between each exon of the coding sequence and the genome assembly. We considered a gene to be duplicated in females if at least 25% of the parent coding sequence aligned to more than one location in the genome assembly.

***S-Lap1* and *GAPsec* gene trees and Y chromosome gene copies**

The Muller-D copies of *S-Lap1* and *GAPsec* were identified in the 12 Drosophila genomes (Drosophila 12 Genomes Consortium *et al.* 2007) by synteny with *D. melanogaster* and their coding sequences were downloaded from FlyBase (Gramates *et al.* 2017). The PRANK software package (Löytynoja 2014) was used to generate codon-aware alignments of coding sequences for each gene. The resulting alignment was trimmed using trimAl (Capella-Gutiérrez *et al.* 2009) and RaxML (Stamatakis 2014) was used to infer a maximum likelihood phylogeny (100 bootstrap replicates). *D. pseudoobscura* Y-linked contigs were identified using read coverage information from male versus female genomic sequencing data. Exonerate (Slater and Birney 2005) was used to determine the location of the amplified copies of *S-Lap1* and *GAPsec* on these scaffolds with the *D. pseudoobscura S-Lap1* (*FBpp0285960*) and *GAPsec* (*FBpp0308917*) peptide sequences as queries. The *D. pseudoobscura* Y copies of each gene were aligned using MAFFT (Katoh and Standley 2013), trimmed with trimAl (Capella-Gutiérrez *et al.* 2009), and a Y consensus sequence for each gene was generated using PILER (Edgar and Myers 2005).

RNA Interference Design

To knockdown the Y-linked copies of *S-Lap1* but not the X-linked copies, we targeted a region on the 3' end of the gene with high divergence between the Y and X copies for specificity, but high similarity between the Y-copies to maximize knockdown. This target sequence was used to design a hairpin using the pVALIUM20 design (Ni *et al.* 2011). We ordered a synthesized construct cloned into pUC57 (Genscript, Piscataway, NJ). The synthesized region contained the hairpin inserted into a small region of the pVALIUM20 plasmid, as well as 1kb of promoter sequence upstream of the *D. pseudoobscura* ortholog of β-tubulin at 85D, *GA21728*. We chose this promoter because both the *D. melanogaster* and *D. pseudoobscura* orthologs are highly, and specifically, expressed in the testis. This synthesized segment was amplified from the pUC57 carrier plasmid by PCR and was cloned into the pCaSpeR4 backbone by Gibson Assembly (**Figure S4**). pCaSpeR4 contains elements suitable for P-element insertion into the *D. pseudoobscura* genome.

bioRxiv preprint doi: https://doi.org/10.1101/324368; this version posted May 16, 2018. The copyright holder for this preprint (which was not certified by peer review) is the author/funder, who has granted bioRxiv a license to display the preprint in perpetuity. It is made available under aCC-BY 4.0 International license.

Transgenic Fly Creation

To create transgenic strains, the RNAi plasmid and a plasmid encoding the Δ2,3 transposase were co-injected into the *white* mutant *D. pseudoobscura* embryos (UCSD Stock Center: 14011-0121.12) by Rainbow Transgenic Flies, Inc. (Camarillo, CA). Following injection, we backcrossed potential transformants to the *D. pseudoobscura white* mutant line. We isolated successful genome integrations in F1 progeny using eye color as a marker of insertion, as pCaSpeR4 contains the *D. melanogaste*r mini-*white* gene, which can successfully rescue eye coloration in *D. pseudoobscura*. We backcrossed transgenic hits to the *white* mutant line, and established two independent stocks of the mutants for phenotypic analysis and imaging studies (*P{w$^+$:sh-S-Lap1-Y}* 1 and *P{w$^+$:sh-S-Lap1-Y}*2).

Crosses to determine sex ratio

To generate experimental and control males to assay progeny sex ratio, virgin *w, P{w$^+$:sh-S- Lap1-Y}* females were crossed with *w* males. Red-eyed *w, P{w$^+$:sh-S-Lap1-Y}* virgin female progeny were selected and crossed to *w, P{w$^+$:sh-S- Lap1-Y}* progeny males. Red-eyed *w, P{w$^+$:sh-S- Lap1-Y}* male progeny, and control *w* male progeny were selected to assay for sex ratio. To assay sex ratio, a single male aged 1-7 days old was crossed to five virgin *w* females aged 1-7 days old and allowed to mate for 10 days. After 10 days, flies were removed, and vials were plugged with a cotton dental roll and moistened with a 0.5% propionic acid solution. All emerging progeny were sexed and counted for 21 days following the first progeny emergence.

RNA libraries and mapping

We dissected testes from 3-8 day old virgin males of *D. pseudoobscura* (strain MV25, transgenic *P{w$^+$:sh-S-Lap1-Y}* and *white* control males) reared at 18°C on Bloomington food. We used Trizol (Invitrogen) and GlycoBlue (Invitrogen) to extract and isolate total RNA. *D. pseudoobscura* CAGE-seq data were obtained from the ModEncode project (Chen *et al.* 2014). We resolved 20 μg of total RNA on a 15% TBE-Urea gel (Invitrogen) and size selected 19-29 nt long RNA, and used Illumina's TruSeq Small RNA Library Preparation Kit to prepare small RNA libraries, which were sequenced on an Illumina HiSeq 4000 at 50 nt read length (single-end)., We used to Ribo-Zero to deplete ribosomal RNA from total RNA, and used Illumina's TruSeq Stranded Total RNA Library Preparation Kit to prepare stranded testis RNA libraries, which were sequenced on an Illumina HiSeq 4000 at 100 nt read length (paired-end). Total RNA data were aligned to the *D. pseudoobscura* reference genome using HISAT2 (Kim *et al.* 2015), whereas Bowtie2 (Langmead and Salzberg 2012) (seed length: 18) was used to align small RNA and CAGE-seq data. In all cases, alignments with mapping quality less than 20 were discarded.

Embryo Lethality Experiment:

For the control experiment, *D. pseudoobscura w* virgin females were crossed to *D. pseudoobscura w* males. For the experimental transgenic experiment, *D. pseudoobscura w* virgin females were crossed with transgenic *w, P(sh-SLap)* males. Flies were placed in an embryo collection chamber with a molasses agar collection plate smeared with regular baker's yeast paste. Flies were allowed to acclimate to the collection chamber for 48 hours. Flies were then given a new agar plate smeared with fresh yeast paste every two hours to lay eggs on. Eggs were allowed to develop for 48 hours, after which all hatched, white unhatched and brown lethal eggs were counted.

bioRxiv preprint doi: https://doi.org/10.1101/324368; this version posted May 16, 2018. The copyright holder for this preprint (which was not certified by peer review) is the author/funder, who has granted bioRxiv a license to display the preprint in perpetuity. It is made available under aCC-BY 4.0 International license.

Sperm isolation and quantification by qPCR

We quantified the number of Y-linked sperm in transgenic *P{w$^+$:sh-S-Lap1-Y}* and *white* control males using qPCR. Sperm was isolated by squeezing them out from dissected seminal vesicles in 1x PBS (**Figure S6**). Sperm from multiple males (4-6 males) were pooled, and we performed 5 independent DNA extractions for transgenic flies and control males each. To extract DNA from sperm, we added 1/10 volumes 10% SDS and 1 volume phenol:chloroform:isoamyl alcohol (25:24:1), centrifuged for five minutes and transferred the upper phase to a new tube. To this, we added 1/10 volumes 3M sodium acetate, 1.25 µl GlycoBlue and 2-3 volumes cold 100% ethanol and precipitated the DNA overnight at -20°C, followed by two 70% ethanol washes. The DNA was resuspended in water. qPCR was performed with the KAPA SYBR® Fast qPCR Master Mix with 2-step cycling (annealing and extension at 60°C). The following primers were used for qPCR: Y-linked gene GA25497 (for: CCGTCCCTGAGATTGCAAGA, rev: TGCAGAGCGAAGGAATAGCC); autosomal control gene GA30136 (for: CACAAAGTCGCCAACAAAGA rev: TGTTGGCATCGGTATAGCTG). We used the $\Delta\Delta C_t$ calculation method to compute relative abundance of Y-linked sperm in transgenic *P{w$^+$:sh-S-Lap1-Y}* vs. *white* control males from qPCR data, relative to the autosomal control gene. Briefly, abundance of the Y-linked gene target (TAR) is normalized to an autosomal control gene (REF) within the same sample to determine $\Delta C_t = C_t$ (TAR) – C_t (REF). This value is exponentially transformed to infer differences in abundance ($2^{-\Delta Ct}$), and normalized to treatment control (i.e. *white* males, $\Delta\Delta C_t$).

Testis Imaging

To examine spermatogenesis in the driving RNAi mutants, we dissected testes from 1-3 day old heterozygous males and fixed the tissues in 4% paraformaldehyde in 1x Phosphate Buffered Saline (PBS) for 1 hour at room temperature. While the fixation protocol was able to clear the majority of the red coloration from the *D. pseudoobscura* testis, some remained. The tissues were rinsed three times with 1x PBS to clear the fixation reagents, then stained with 1µM TO-PRO3, which emits in the far-red spectrum. This fluor, unlike those that emit in the green or red portions of the spectrum, can be visualized through the *D. pseudoobscura* testis coloration with relative clarity. We imaged these testes by confocal microscopy using a Zeiss LSM 880, at both 200x and 630x magnification. Images were adjusted for brightness and contrast, and the seminal vesicles attached to the testes were cropped out of the image. To prepare samples for electron microscopy, we dissected testes from 1-3 day old males and fixed them at 4 degrees C for 24 hours (1% glutaraldehyde, 2.5% paraformaldehyde, 6mM $CaCl_2$, 4.8% sucrose, 100mM cacodylate buffer pH 7.4). The Electron Microscopy Core at the University of Utah (Salt Lake City, UT) stained and sectioned the tissues. The samples were secondarily fixed at room temperature for 1 hour (2% osmium tetroxide in cacodylate buffer) and stained with saturated uranyl acetate at room temperature for 1 hour, then dehydrated and infiltrated with epoxy resin. Samples were polymerized at 60 degrees C for 48 hours, then sectioned for transmission electron microscopy. We imaged these slices using a Hitachi H-7100 TEM electron microscope at 125keV, 2500x. Images were adjusted for brightness and contrast and cropped to contain a single cyst.

References:

Bachtrog D., 2013 Y-chromosome evolution: emerging insights into processes of Y-chromosome degeneration. Nat. Rev. Genet. **14**: 113–124.

Bachtrog D., Mank J. E., Peichel C. L., Kirkpatrick M., Otto S. P., Ashman T.-L., Hahn M. W., Kitano J., Mayrose I., Ming R.,

bioRxiv preprint doi: https://doi.org/10.1101/324368; this version posted May 16, 2018. The copyright holder for this preprint (which was not certified by peer review) is the author/funder, who has granted bioRxiv a license to display the preprint in perpetuity. It is made available under aCC-BY 4.0 International license.

Perrin N., Ross L., Valenzuela N., Vamosi J. C., Tree of Sex Consortium, 2014 Sex determination: why so many ways of doing it? PLoS Biol. **12**: e1001899.

Balakireva M. D., Shevelyov YuYa, Nurminsky D. I., Livak K. J., Gvozdev V. A., 1992 Structural organization and diversification of Y-linked sequences comprising Su(Ste) genes in Drosophila melanogaster. Nucleic Acids Res. **20**: 3731–3736.

Buchfink B., Xie C., Huson D. H., 2015 Fast and sensitive protein alignment using DIAMOND. Nat. Methods **12**: 59–60.

Camacho C., Coulouris G., Avagyan V., Ma N., Papadopoulos J., Bealer K., Madden T. L., 2009 BLAST+: architecture and applications. BMC Bioinformatics **10**: 421.

Capella-Gutiérrez S., Silla-Martínez J. M., Gabaldón T., 2009 trimAl: a tool for automated alignment trimming in large-scale phylogenetic analyses. Bioinformatics **25**: 1972–1973.

Chen Z.-X., Sturgill D., Qu J., Jiang H., Park S., Boley N., Suzuki A. M., Fletcher A. R., Plachetzki D. C., FitzGerald P. C., Artieri C. G., Atallah J., Barmina O., Brown J. B., Blankenburg K. P., Clough E., Dasgupta A., Gubbala S., Han Y., Jayaseelan J. C., Kalra D., Kim Y.-A., Kovar C. L., Lee S. L., Li M., Malley J. D., Malone J. H., Mathew T., Mattiuzzo N. R., Munidasa M., Muzny D. M., Ongeri F., Perales L., Przytycka T. M., Pu L.-L., Robinson G., Thornton R. L., Saada N., Scherer S. E., Smith H. E., Vinson C., Warner C. B., Worley K. C., Wu Y.-Q., Zou X., Cherbas P., Kellis M., Eisen M. B., Piano F., Kionte K., Fitch D. H., Sternberg P. W., Cutter A. D., Duff M. O., Hoskins R. A., Graveley B. R., Gibbs R. A., Bickel P. J., Kopp A., Carninci P., Celniker S. E., Oliver B., Richards S., 2014 Comparative validation of the D. melanogaster modENCODE transcriptome annotation. Genome Res. **24**: 1209–1223.

Cocquet J., Ellis P. J. I., Mahadevaiah S. K., Affara N. A., Vaiman D., Burgoyne P. S., 2012 A genetic basis for a postmeiotic X versus Y chromosome intragenomic conflict in the mouse. (MW Nachman, Ed.). PLoS Genet. **8**: e1002900.

Cocquet J., Ellis P. J. I., Yamauchi Y., Mahadevaiah S. K., Affara N. A., Ward M. A., Burgoyne P. S., 2009 The multicopy gene Sly represses the sex chromosomes in the male mouse germline after meiosis. (N Hastie, Ed.). PLoS Biol. **7**: e1000244.

Dorus S., Wilkin E. C., Karr T. L., 2011 Expansion and functional diversification of a leucyl aminopeptidase family that encodes the major protein constituents of Drosophila sperm. BMC Genomics **12**: 177.

Drosophila 12 Genomes Consortium, , 2007 Evolution of genes and genomes on the Drosophila phylogeny. Nature **450**: 203–218.

Edgar R. C., Myers E. W., 2005 PILER: identification and classification of genomic repeats. Bioinformatics **21 Suppl 1**: i152–8.

Emerson J. J., Kaessmann H., Betrán E., Long M., 2004 Extensive gene traffic on the mammalian X chromosome. Science **303**: 537–540.

Frank S. A., 1991 DIVERGENCE OF MEIOTIC DRIVE-SUPPRESSION SYSTEMS AS AN EXPLANATION FOR SEX-BIASED HYBRID STERILITY AND INVIABILITY. Evolution **45**: 262–267.

Gramates L. S., Marygold S. J., Santos G. D., Urbano J.-M., Antonazzo G., Matthews B. B., Rey A. J., Tabone C. J., Crosby M. A., Emmert D. B., Falls K., Goodman J. L., Hu Y., Ponting L., Schroeder A. J., Strelets V. B., Thurmond J., Zhou P., the FlyBase Consortium, 2017 FlyBase at 25: looking to the future. Nucleic Acids Res. **45**: D663–D671.

Hurst G. D., Werren J. H., 2001 The role of selfish genetic elements in eukaryotic evolution. Nat. Rev. Genet. **2**: 597–606.

Hurst L. D., Pomiankowski A., 1991 Causes of sex ratio bias may account for unisexual sterility in hybrids: a new explanation of Haldane's rule and related phenomena. Genetics **128**: 841–858.

Jaenike J., 2003 Sex Chromosome Meiotic Drive. http://dx.doi.org/10.1146/annurev.ecolsys.32.081501.113958 **32**: 25–49.

Katoh K., Standley D. M., 2013 MAFFT multiple sequence alignment software version 7: improvements in performance and usability. Mol. Biol. Evol. **30**: 772–780.

bioRxiv preprint doi: https://doi.org/10.1101/324368; this version posted May 16, 2018. The copyright holder for this preprint (which was not certified by peer review) is the author/funder, who has granted bioRxiv a license to display the preprint in perpetuity. It is made available under aCC-BY 4.0 International license.

Kim D., Langmead B., Salzberg S. L., 2015 HISAT: a fast spliced aligner with low memory requirements. Nat. Methods **12**: 357–360.

Langmead B., Salzberg S. L., 2012 Fast gapped-read alignment with Bowtie 2. Nat. Methods **9**: 357–359.

Li H., 2015 BFC: correcting Illumina sequencing errors. Bioinformatics **31**: 2885–2887.

Lindholm A. K., Dyer K. A., Firman R. C., Fishman L., Forstmeier W., Holman L., Johannesson H., Knief U., Kokko H., Larracuente A. M., Manser A., Montchamp-Moreau C., Petrosyan V. G., Pomiankowski A., Presgraves D. C., Safronova L. D., Sutter A., Unckless R. L., Verspoor R. L., Wedell N., Wilkinson G. S., Price T. A. R., 2016 The Ecology and Evolutionary Dynamics of Meiotic Drive. Trends Ecol. Evol. (Amst.) **31**: 315–326.

Löytynoja A., 2014 Phylogeny-aware alignment with PRANK. Methods Mol. Biol. **1079**: 155–170.

Lucchesi J. C., 1978 Gene dosage compensation and the evolution of sex chromosomes. Science **202**: 711–716.

McDermott S. R., Noor M. A. F., 2010 The role of meiotic drive in hybrid male sterility. Philos. Trans. R. Soc. Lond., B, Biol. Sci. **365**: 1265–1272.

Meiklejohn C. D., Tao Y., 2010 Genetic conflict and sex chromosome evolution. Trends Ecol. Evol. (Amst.) **25**: 215–223.

Merrill C., 1999 Truncated RanGAP Encoded by the Segregation Distorter Locus of Drosophila. Science **283**: 1742–1745.

Ni J.-Q., Zhou R., Czech B., Liu L.-P., Holderbaum L., Yang-Zhou D., Shim H.-S., Tao R., Handler D., Karpowicz P., Binari R., Booker M., Brennecke J., Perkins L. A., Hannon G. J., Perrimon N., 2011 A genome-scale shRNA resource for transgenic RNAi in Drosophila. Nat. Methods **8**: 405–407.

Peng Y., Leung H. C. M., Yiu S. M., Chin F. Y. L., 2012 IDBA-UD: a de novo assembler for single-cell and metagenomic sequencing data with highly uneven depth. Bioinformatics **28**: 1420–1428.

Policansky D., Ellison J., 1970 “Sex ratio” in Drosophila pseudoobscura: spermiogenic failure. Science **169**: 888–889.

Presgraves D. C., 2010 The molecular evolutionary basis of species formation. Nat. Rev. Genet. **11**: 175–180.

Sandler L., Novitski E., 1957 Meiotic Drive as an Evolutionary Force. The American Naturalist **91**: 105–110.

Slater G. S. C., Birney E., 2005 Automated generation of heuristics for biological sequence comparison. BMC Bioinformatics **6**: 31.

Soh Y. Q. S., Alföldi J., Pyntikova T., Brown L. G., Graves T., Minx P. J., Fulton R. S., Kremitzki C., Koutseva N., Mueller J. L., Rozen S., Hughes J. F., Owens E., Womack J. E., Murphy W. J., Cao Q., de Jong P., Warren W. C., Wilson R. K., Skaletsky H., Page D. C., 2014 Sequencing the mouse Y chromosome reveals convergent gene acquisition and amplification on both sex chromosomes. Cell **159**: 800–813.

Stamatakis A., 2014 RAxML version 8: a tool for phylogenetic analysis and post-analysis of large phylogenies. Bioinformatics **30**: 1312–1313.

Tao Y., Araripe L., Kingan S. B., Ke Y., Xiao H., Hartl D. L., 2007a A sex-ratio Meiotic Drive System in Drosophila simulans. II: An X-linked Distorter (D Barbash, Ed.). PLoS Biol. **5**: e293.

Tao Y., Masly J. P., Araripe L., Ke Y., Hartl D. L., 2007b A sex-ratio meiotic drive system in Drosophila simulans. I: an autosomal suppressor. (D Barbash, Ed.). PLoS Biol. **5**: e292.

Vibranovski M. D., Zhang Y., Long M., 2009 General gene movement off the X chromosome in the Drosophila genus. Genome Res. **19**: 897–903.

bioRxiv preprint doi: https://doi.org/10.1101/324368; this version posted May 16, 2018. The copyright holder for this preprint (which was not certified by peer review) is the author/funder, who has granted bioRxiv a license to display the preprint in perpetuity. It is made available under aCC-BY 4.0 International license.

Vicoso B., Bachtrog D., 2013 Reversal of an ancient sex chromosome to an autosome in Drosophila. Nature **499**: 332–335.

Wen J., Duan H., Bejarano F., Okamura K., Fabian L., Brill J. A., Bortolamiol-Becet D., Martin R., Ruby J. G., Lai E. C., 2015 Adaptive regulation of testis gene expression and control of male fertility by the Drosophila hairpin RNA pathway. [Corrected]. Mol. Cell **57**: 165–178.

Zhang L., Sun T., Woldesellassie F., Xiao H., Tao Y., 2015 Sex ratio meiotic drive as a plausible evolutionary mechanism for hybrid male sterility. (DJ Begun, Ed.). PLoS Genet. **11**: e1005073.

Acknowledgements Funded by NIH grants (R01GM076007, GM101255 and R01GM093182) to DB, 5T32GM007464-40 (CL), and R01 GM115914 (NP) and the Pew Scholars Program (NP).

Author contributions. C.E. generated the genome data and performed the bioinformatics analysis. C.L. and N.P. created the transgenic flies and performed imaging analysis, E.L. performed the phenotypic assays, L.G. generated RNA libraries and D.B. oversaw the project and wrote the manuscript with input from all authors.

Competing interests: The authors declare that no competing interests exist.

Figure Legends

Figure 1. **Molecular evolution of the *S-Lap1* and *GAPsec* genes in Drosophila**. **A.** Organization of *S-Lap1* and *GAPsec* genes across the Drosophila genus. *S-Lap1* is duplicated in all Drosophila species investigated, and *GAPsec* shows a partial duplication in *D. pseudoobscura* and its sister species *D. persimilis*. **B.** Amplification of *S-Lap1* and *GAPsec* on Y-linked scaffolds of *D. pseudoobscura*. **C.** Gene trees of *S-Lap1* and *GAPsec* copies. *S-Lap1* independently duplicated multiple times across the Drosophila phylogeny. Inferred duplication events are shown by the yellow circle.

Figure 2. Knockdown of Y-linked *S-Lap1* copies reveals a cryptic meiotic drive. A. *S-Lap1*-Y RNAi targets diverged region between X and Y-linked gene copies. The hairpin targets a region of the gene that contains five polymorphic sites between X and Y copies of *S-Lap1*. This region is also conserved among Y-linked copies of this gene, and targets a region on the last exon of *S-Lap1*. **B.** Knockdown of Y-linked *S-Lap1* (P[w+;sh-SLAP]2) results in female-biased offspring to control males (*white* control). Shown are total male and female progeny counts of transgenic males from two independent insertions of the *S-Lap1*-Y RNAi construct (P[w+;sh-SLAP]1 and P[w+;sh-SLAP]2), compared to control males (*white* control). Both transgenic lines show a highly female-biased offspring sex ratio (66% and 89%). **C.** Knockdown of Y-linked *S-Lap1* (P[w+;sh-SLAP]2) results in fewer Y-linked sperm compared to *white* control males (~25% fewer Y-sperm; *P*=0.02; t-test). Shown is quantification of genomic sperm DNA with qPCR using a Y-linked vs. an autosomal primer for *S-Lap1*-Y depleted flies versus *white* control flies.

Figure 3. *S-Lap1*-Y knockdown in the testis leads to spermatogenesis defects and segregation distortion. A. In wild-type testes, spermatogenesis begins with mitotic and meiotic cell divisions in the upper region of the testis, before proceeding to sperm maturation. Cysts are neatly ordered and DNA is compacted. In *the S-Lap1*-Y knockdown testes, nuclei are disordered

bioRxiv preprint doi: https://doi.org/10.1101/324368; this version posted May 16, 2018. The copyright holder for this preprint (which was not certified by peer review) is the author/funder, who has granted bioRxiv a license to display the preprint in perpetuity. It is made available under aCC-BY 4.0 International license.

and improperly condensed, and very few cysts are undergoing the sperm maturation process. **B.** *S-Lap1*-Y knockdown cysts with maturing sperm contain nuclei with different compaction states, in contrast to wild-type testes. Knockdown cysts contain both needle-shaped and oval sperm within a single bundle, while similarly-developed cysts in the wildtype contain only sperm with needle-shaped nuclei, indicating that development is proceeding unevenly in the knockdown testes. **C.** In electron micrographs of wild-type sperm, cysts late in development contain 128 sperm in each bundle, while in the *S-Lap1*-Y knockdown cysts there are far fewer developing sperm in each cyst. Scale bars: *(A)* 200µm, *(B)* 20 µm, *(C)* 1 µm.

Figure 4. Short RNA's may be involved in suppression of the cryptic *S-Lap1* drive system. A. Expression and short RNA profiles from wildtype *D. pseudoobscura* testis. Stranded RNA-seq (red tracks) reveals that the X-linked copy of *S-Lap1*-duplicate produces both sense and anti-sense transcripts, resulting in the production of short RNA's (blue tracks). CAGE-seq data (grey tracks) support that the *GAPsec* duplicate generated a new TSS resulting in antisense transcript of *S-Lap1*-dup. **B.** A hypothetical evolutionary model of the cryptic *S-Lap1* drive system. *S-Lap1* was duplicated in an ancestor of *D. pseudoobscura*, and a partial duplication of *GAPsec* created a TSS for anti-sense transcription of *S-Lap1* duplicate. Production of small RNA's may deplete *S-Lap1* transcripts, which may result in elimination of Y-bearing sperm, and could be compensated by amplification of *S-Lap1* on the Y chromosome.

Table 1. Multi-copy Y-linked genes across Drosophila species. Shown is which chromosome arms form the neo-sex chromosomes (based on synteny in *D. melanogaster*). Genes in bold have functions related to chromosome segregation.

Figure S1. **Inference of sex chromosomes using male and female coverage data**. Plotted is the normalized male / female genomic read coverage for scaffolds mapped to the *D. melanogaster* genome, to infer the location of Muller elements.

Figure S2. **Validation of bioinformatics pipeline to infer multi-copy Y genes in *D. pseudoobscura***. Shown is the predicted coverage based on mapping of Illumina reads on the x-axis, versus the number of Y-linked copies of a gene found in the genome assembly. Note that our bioinformatics pipeline is conservative and underestimates the number of Y-linked copies found in the assembly, presumably due to many multi-copy genes being fragmented in the assembly.

Figure S3. **Phylogeny of *S-Lap1* and *GAPsec* gene families in *D. pseudoobscura***.

Figure S4. **Vector design for *S-Lap1*-Y knockdown**.

Figure S5. **Crossing design for assaying meiotic drive sex ratio.** Red-eyed *w; P(sh-S-LAP2)* virgin females were crossed to *w* males. The transgenes were determined to be X-linked based on progeny eye color. Red-eyed *w, P{sh-S-LAP2}* virgin female progeny were selected and crossed to *w, P{sh-S-LAP2}* progeny males. To assay sex ratio, 1-7 day old individual red-eyed *w; P(sh-S-LAP2)* males and 1-7 day old individual control *w* males were selected and crossed to five 1-7 day old virgin *w* females.

Figure S6. Testes and seminal vesicle dissections and sperm isolation. A. Testes and seminal vesicles were isolated, and

bioRxiv preprint doi: https://doi.org/10.1101/324368; this version posted May 16, 2018. The copyright holder for this preprint (which was not certified by peer review) is the author/funder, who has granted bioRxiv a license to display the preprint in perpetuity. It is made available under aCC-BY 4.0 International license.

connecting accessory glands were removed. **B.** Testes were isolated from seminal vesicles to be stored in Trizol for RNA extraction. **C.** Individual seminal vesicles were separated. **D.** Sperm was isolated from seminal vesicle by removing the encasing sheath, and stored in PBS for DNA extraction.

Table S1. Species used in this study. Shown are species and stock numbers, total assembly size, and sex chromosome karyotype (see Figure S1).

Table S2. Multi-copy Y-linked genes across Drosophila species. Shown are the orthologous location of multi-copy Y genes in *D. melanogaster*, and their inferred molecular function and gene expression pattern in *D. melanogaster* (data from flybase.org).

Table S3. **Down-regulation of Y-linked copies of *S-Lap1* in P[w+;sh-SLAP] flies versus *white* control males.** To avoid cross-mapping of short RNA-seq reads between X and Y-derived transcripts, reads where only mapped to two regions with multiple fixed differences between the X and Y copies (Region_1 and Region_2; Region_2 corresponds to the genomic regions against which the hairpin RNA was designed). Both regions show about a 40% reduction in Y-linked transcripts in testis, compared to control *white* males.

Table S4. Embryonic hatch rates of transgenic P[w+;sh-SLAP] versus *white* control flies. Differences in sex ratio between transgenic and control flies are not caused by male-specific embryonic lethality.

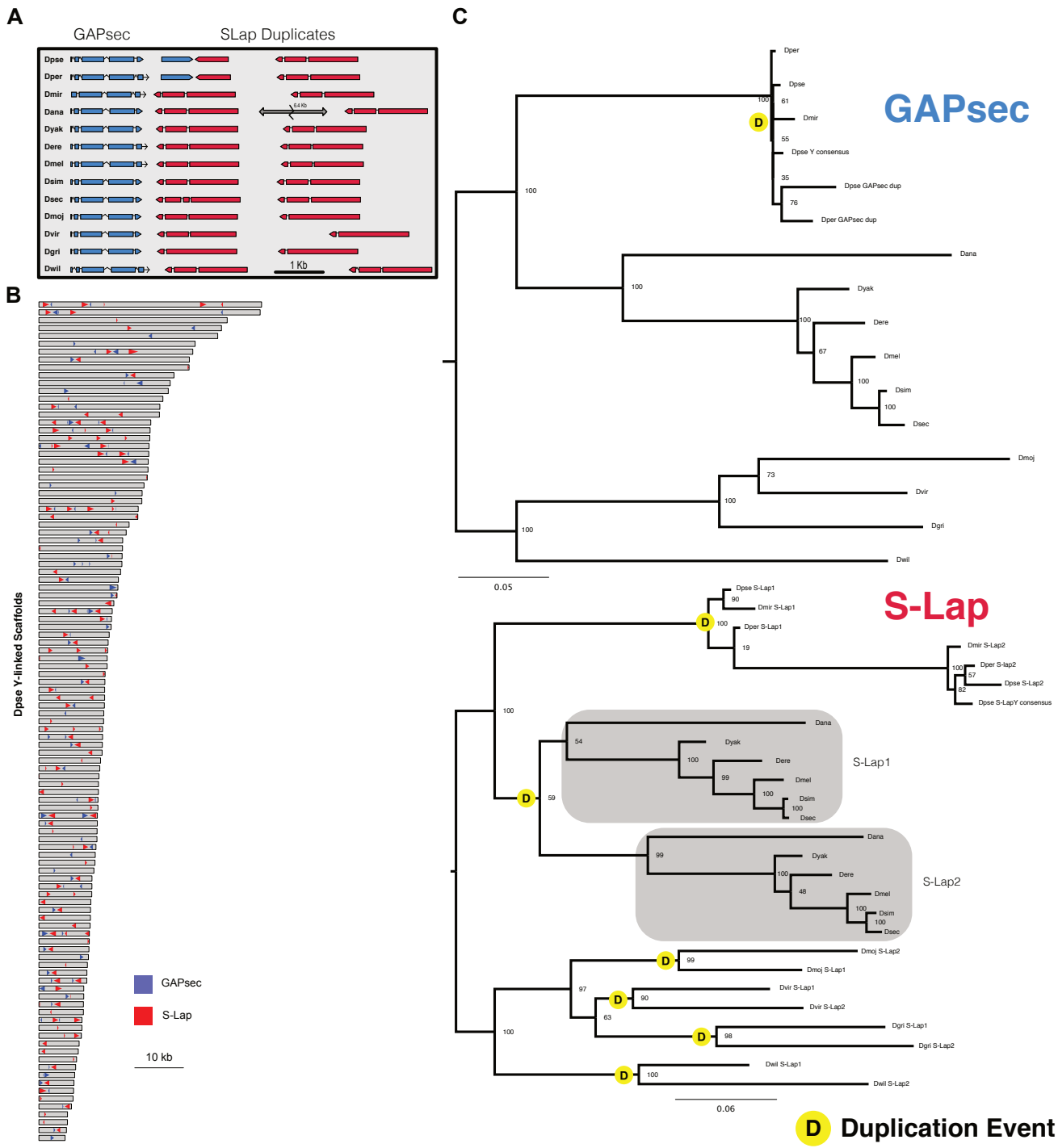

Figure 1. Molecular evolution of the *S-Lap1* and *GAPsec* genes in Drosophila. A. Organization of *S-Lap1* and *GAPsec* genes across the Drosophila genus. *S-Lap1* is duplicated in all Drosophila species investigated, and *GAPsec* shows a partial duplication in *D. pseudoobscura* and its sister species *D. persimilis*. **B.** Amplification of *S-Lap1* and *GAPsec* on Y-linked scaffolds of *D. pseudoobscura*. **C.** Gene trees of *S-Lap1* and *GAPsec* copies. *S-Lap1* independently duplicated multiple times across the Drosophila phylogeny. Inferred duplication events are shown by the yellow circle.

A.

C.

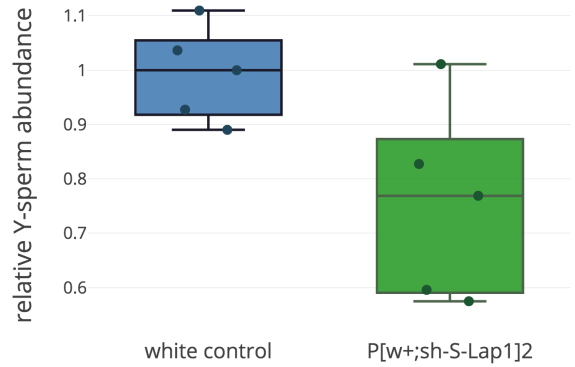

B.

Progeny sex ratios across lines

Parental male genotype	N[a]	Total Male Progeny	Total female progeny	Total Progeny Sex Ratio	Mean Male Progeny	Mean Female Progeny	Mean Sex Ratio	SE	*P*[c]	t	df
P[w+:sh-SLAP2]1	34	2344	4396	0.652	68.941	129.294	0.662	0.029	1.55E-05	-4.9482	38.175
w^b	27	2493	2683	0.518	92.333	99.37	0.515	0.008			
P[w+:sh-SLAP2]2	33	621	3960	0.864	18.818	120	0.891	0.032	1.105E-10	-7.942	54.855
w^b	24	1937	2190	0.530	80.708	91.25	0.551	0.029			

[a] Number of individual males assayed for progeny sex ratio
[b] *w* control brothers from respective crosses
[c] Welch Two Sample t-test

Figure 2. Knockdown of Y-linked *S-Lap1* copies reveals a cryptic meiotic drive. **A.** *S-Lap1*-Y RNAi targets diverged region between X and Y-linked gene copies. The hairpin targets a region of the gene that contains five polymorphic sites between X and Y copies of S-Lap1. This region is also conserved among Y-linked copies of this gene, and targets a region on the last exon of S-Lap1. **B.** Knockdown of Y-linked *S-Lap1* (P[w+;sh-SLAP]2) results in female-biased offspring to control males (*white* control). Shown are total male and female progeny counts of transgenic males from two independent insertions of the *S-Lap1*-Y RNAi construct (P[w+;sh-SLAP]1 and P[w+;sh-SLAP]2), compared to control males (*white* control). Both transgenic lines show a highly female-biased offspring sex ratio (66% and 89%). **C.** Knockdown of Y-linked *S-Lap1* (P[w+;sh-SLAP]2) results in fewer Y-linked sperm compared to *white* control males (~25% fewer Y-sperm; *P*=0.02; t-test). Shown is quantification of genomic sperm DNA with qPCR using a Y-linked vs. an autosomal primer for *S-Lap1*-Y depleted flies versus *white* control flies.

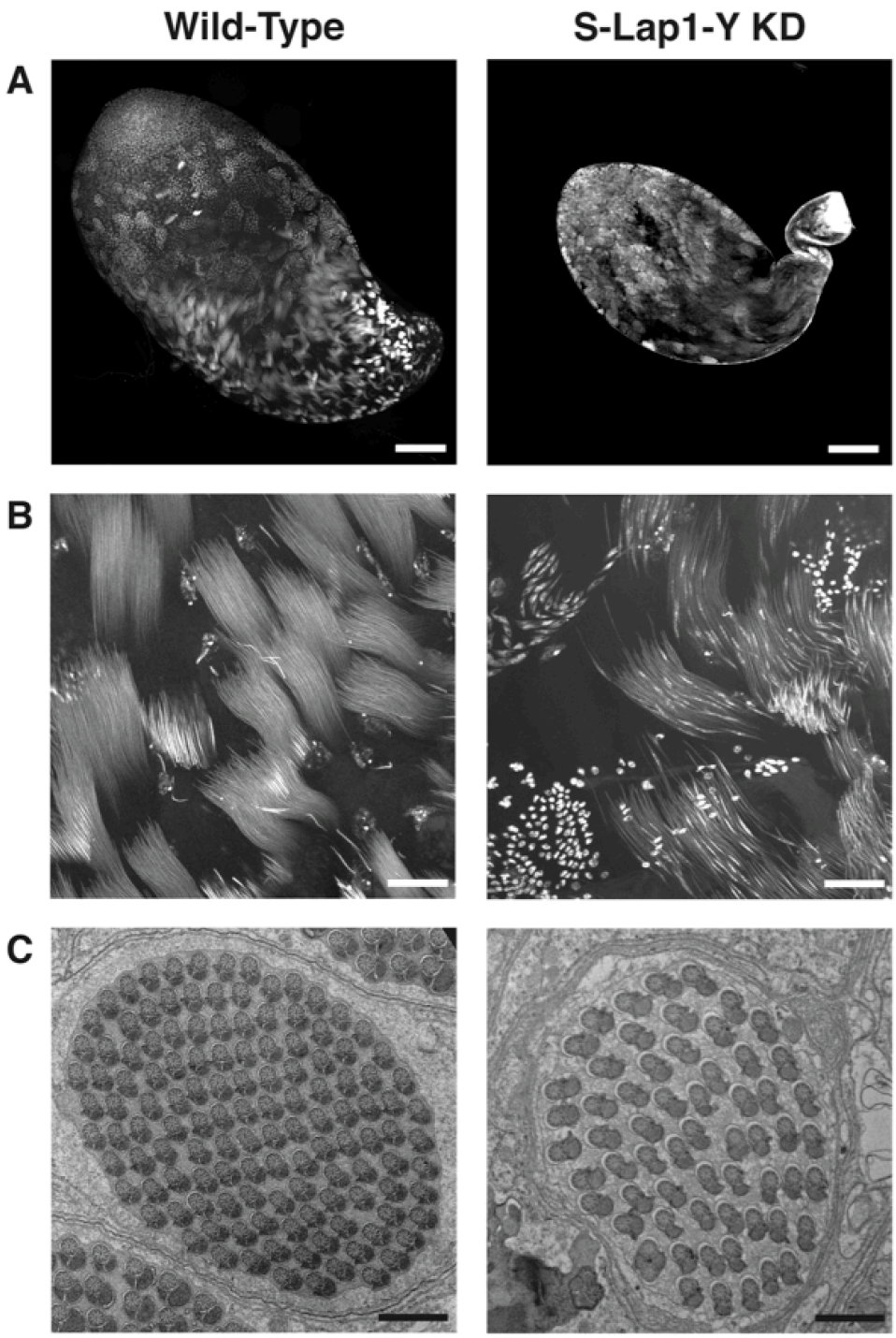

Figure 3. *S-Lap1*-Y knockdown in the testis leads to spermatogenesis defects and segregation distortion. A. In wild-type testes, spermatogenesis begins with mitotic and meiotic cell divisions in the upper region of the testis, before proceeding to sperm maturation. Cysts are neatly ordered and DNA is compacted. In *the S-Lap1*-Y knockdown testes, nuclei are disordered and improperly condensed, and very few cysts are undergoing the sperm maturation process. **B.** *S-Lap1*-Y knockdown cysts with maturing sperm contain nuclei with different compaction states, in contrast to wild-type testes. Knockdown cysts contain both needle-shaped and oval sperm within a single bundle, while similarly-developed cysts in the wildtype contain only sperm with needle-shaped nuclei, indicating that development is proceeding unevenly in the knockdown testes. **C.** In electron micrographs of wild-type sperm, cysts late in development contain 128 sperm in each bundle, while in the *S-Lap1*-Y knockdown cysts there are far fewer developing sperm in each cyst. Scale bars: *(A)* 200µm, *(B)* 20 µm, *(C)* 1 µm.

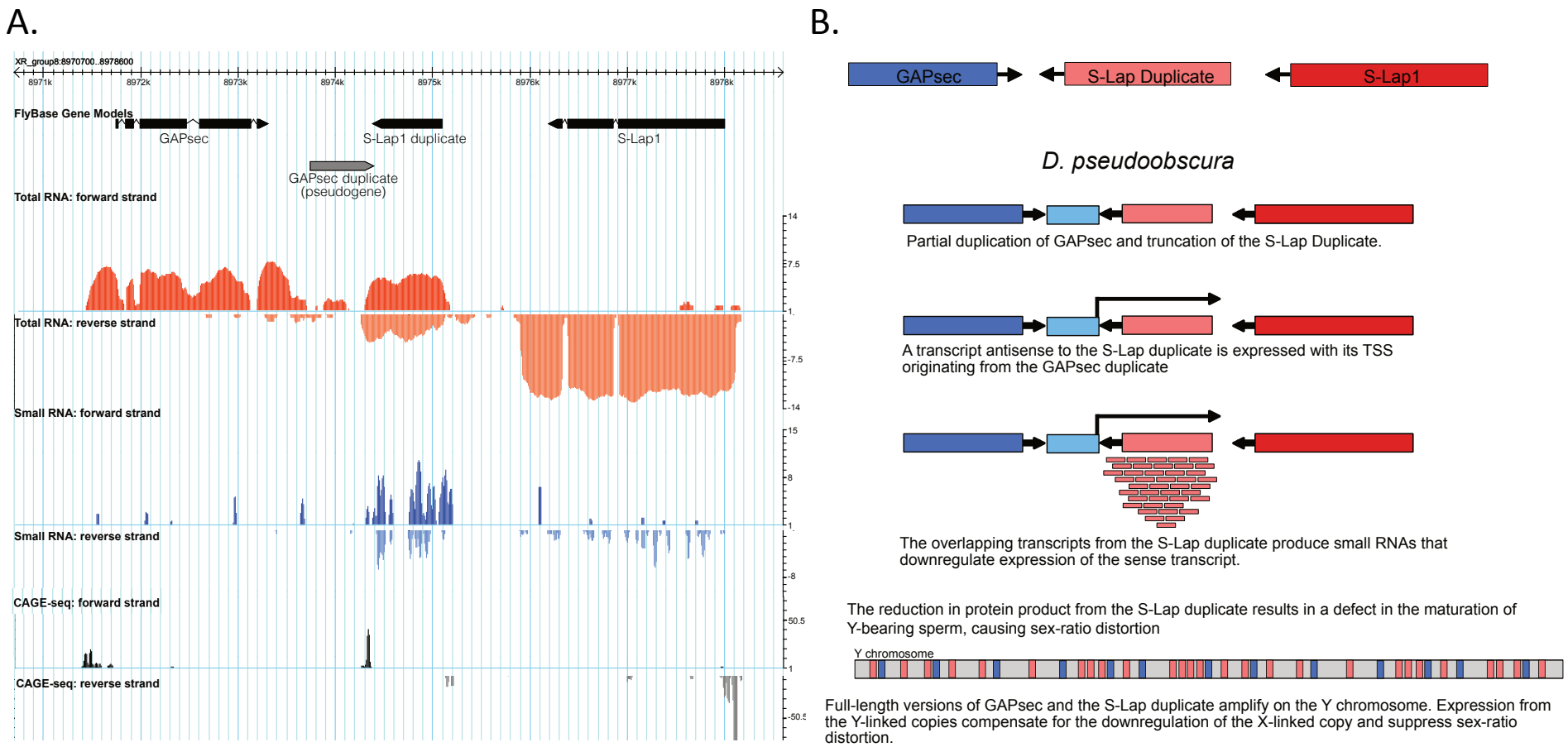

Figure 4. Short RNA's may be involved in suppression of the cryptic *S-Lap1* drive system. A. Expression and short RNA profiles from wildtype *D. pseudoobscura* testis. Stranded RNA-seq (red tracks) reveals that the X-linked copy of *S-Lap1*-duplicate produces both sense and anti-sense transcripts, resulting in the production of short RNA's (blue tracks). CAGE-seq data (grey tracks) support that the *GAPsec* duplicate generated a new TSS resulting in antisense transcript of *S-Lap1*-dup. **B.** A hypothetical evolutionary model of the cryptic *S-Lap1* drive system. *S-Lap1* was duplicated in an ancestor of *D. pseudoobscura*, and a partial duplication of *GAPsec* created a TSS for anti-sense transcription of *S-Lap1* duplicate. Production of small RNA's may deplete *S-Lap1* transcripts, which may result in elimination of Y-bearing sperm, and could be compensated by amplification of *S-Lap1* on the Y chromosome.

Table 1. Multi-copy Y-linked genes across Drosophila species. Shown is which chromosome arms form the neo-sex chromosomes (based on synteny in *D. melanogaster*). Genes in bold have functions related to chromosome segregation.

Species	Neo-sex chromosome	Amplified Y genes
D. albomicans	3L, 2R	FBgn0053725*
D. americana	2L	FBgn0032715*
D. athabasca	3L, 2R	FBgn0045483*, FBgn0034429*, FBgn0034328*, FBgn0036640, FBgn0266456
D. lummei	no	**dhd**#
D. melanica	3L	FBgn0028668*, FBgn0010424*, FBgn0053796*
D. miranda	3L, 2R	FBgn0026582*, FBgn0060296*, **Klp61F**, FBgn0034491*, **PCNA***, **fest***, FBgn0034324*, **thr***, S-Lap5*, **mars***, FBgn0033788*, FBgn0033354*, **scra***, FBgn0033216*, FBgn0054045*, **Drak**#
D. nannoptera	3L	FBgn0031103#
D. nigromelanica	2R	FBgn0063491*, **Iswi***
D. pseudoobscura	3L	S-Lap1*, S-Lap2*, GAPsec*, FBgn0035690*
D. robusta	3L	FBgn00103178, FBgn0046301*, FBgn0053795*

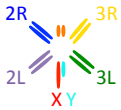

Muller element's

located on ancestral X
* located on neo-sex chromosome

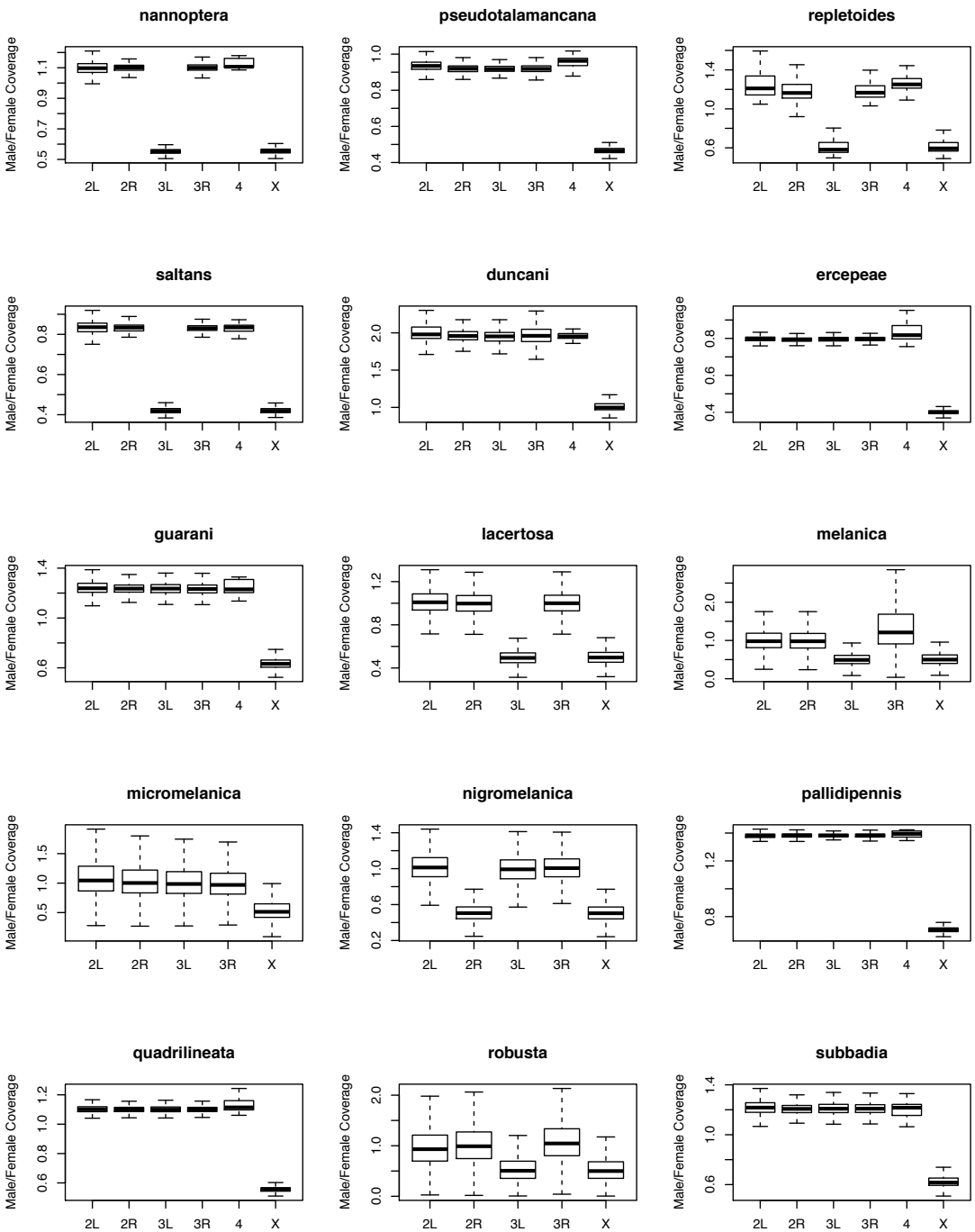

Figure S1. **Inference of sex chromosomes using male and female coverage data.** Plotted is the normalized male / female genomic read coverage for scaffolds mapped to the *D. melanogaster* genome, to infer the location of Muller elements.

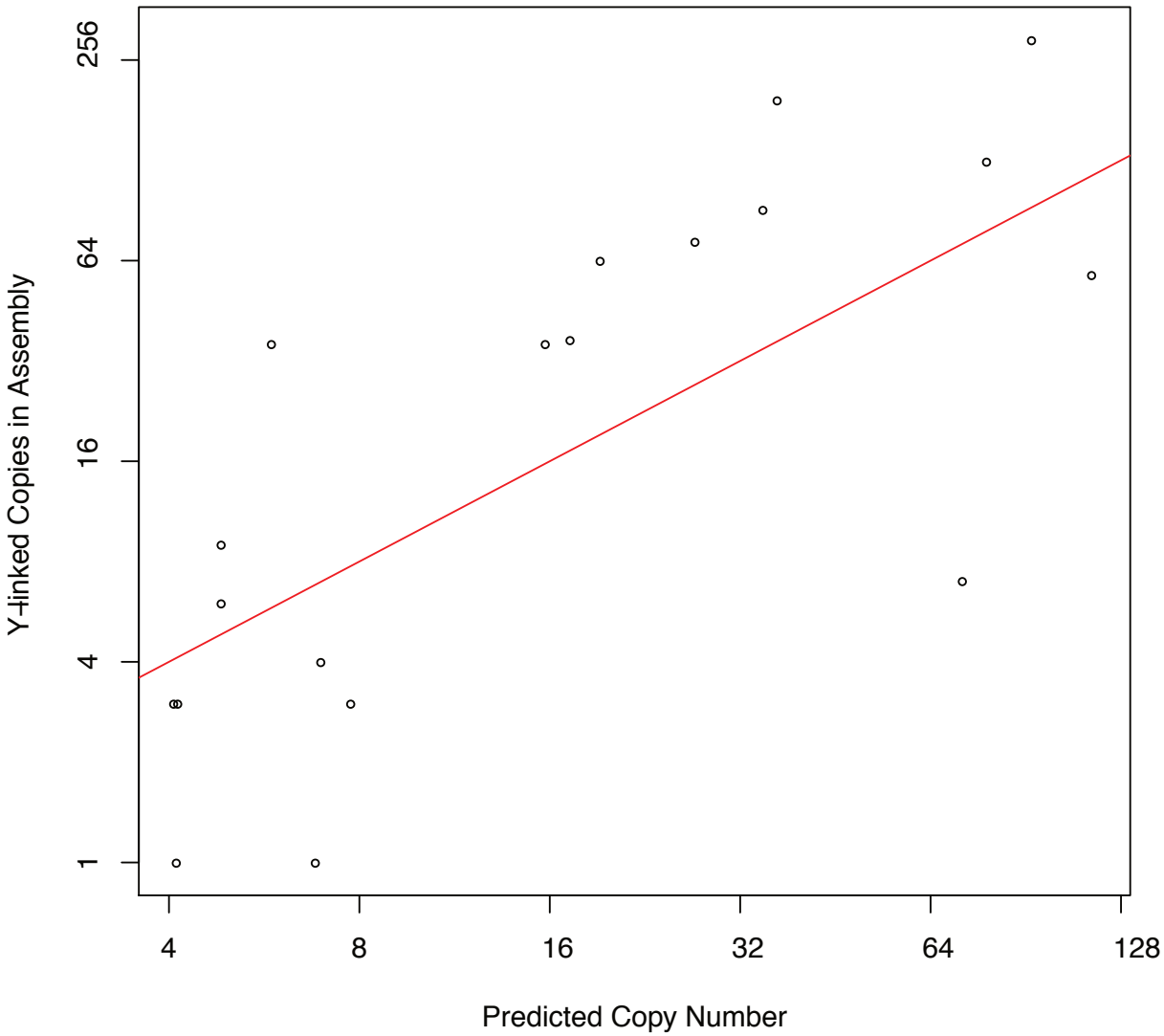

Figure S2. **Validation of bioinformatics pipeline to infer multi-copy Y genes in *D. pseudoobscura***. Shown is the predicted coverage based on mapping of Illumina reads on the x-axis, versus the number of Y-linked copies of a gene found in the genome assembly. Note that our bioinformatics pipeline is conservative and underestimates the number of Y-linked copies found in the assembly, presumably due to many multi-copy genes being fragmented in the assembly.

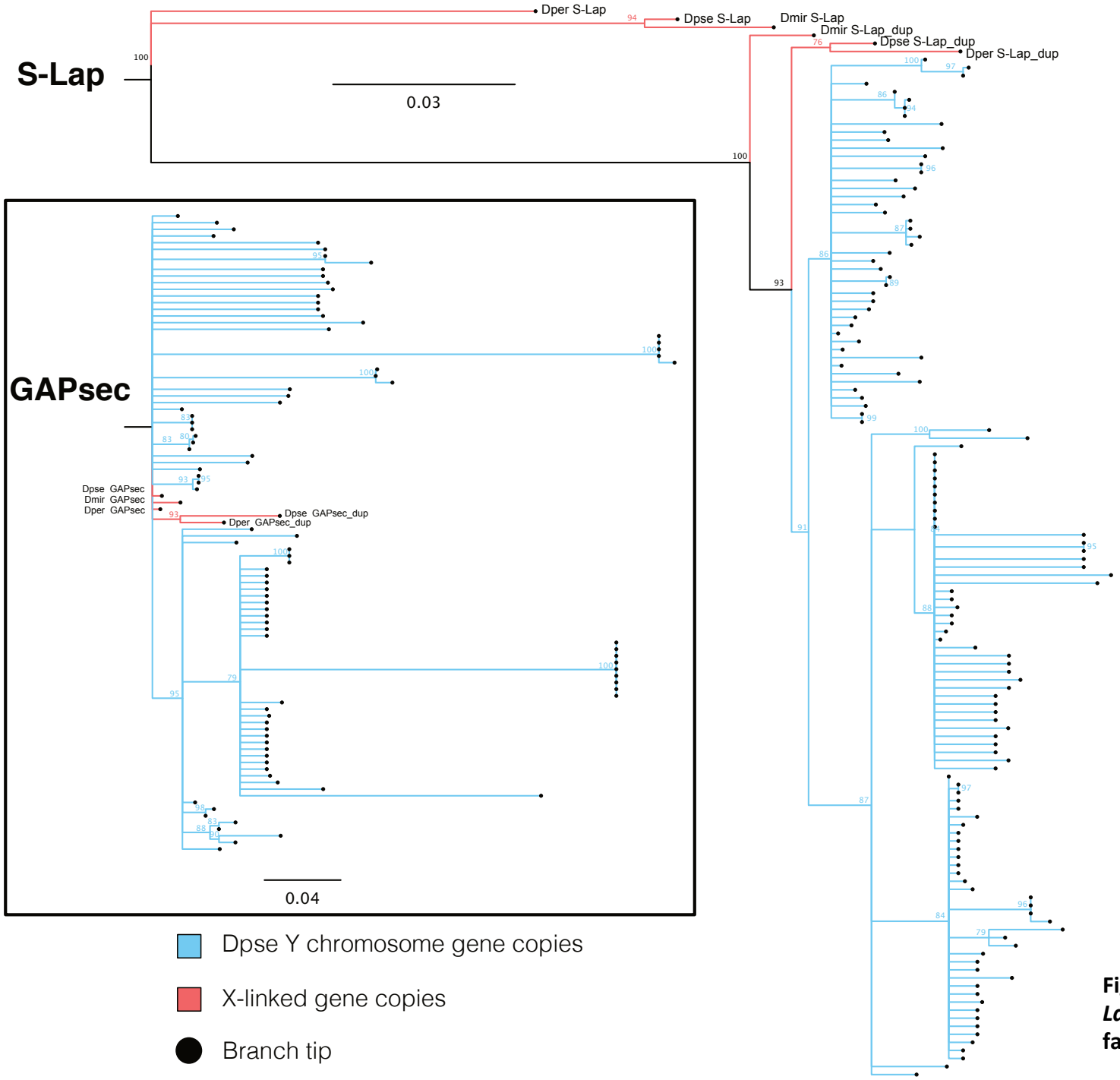

Figure S3. Phylogeny of *S-Lap1* and *GAPsec* gene families in *D. pseudoobscura*.

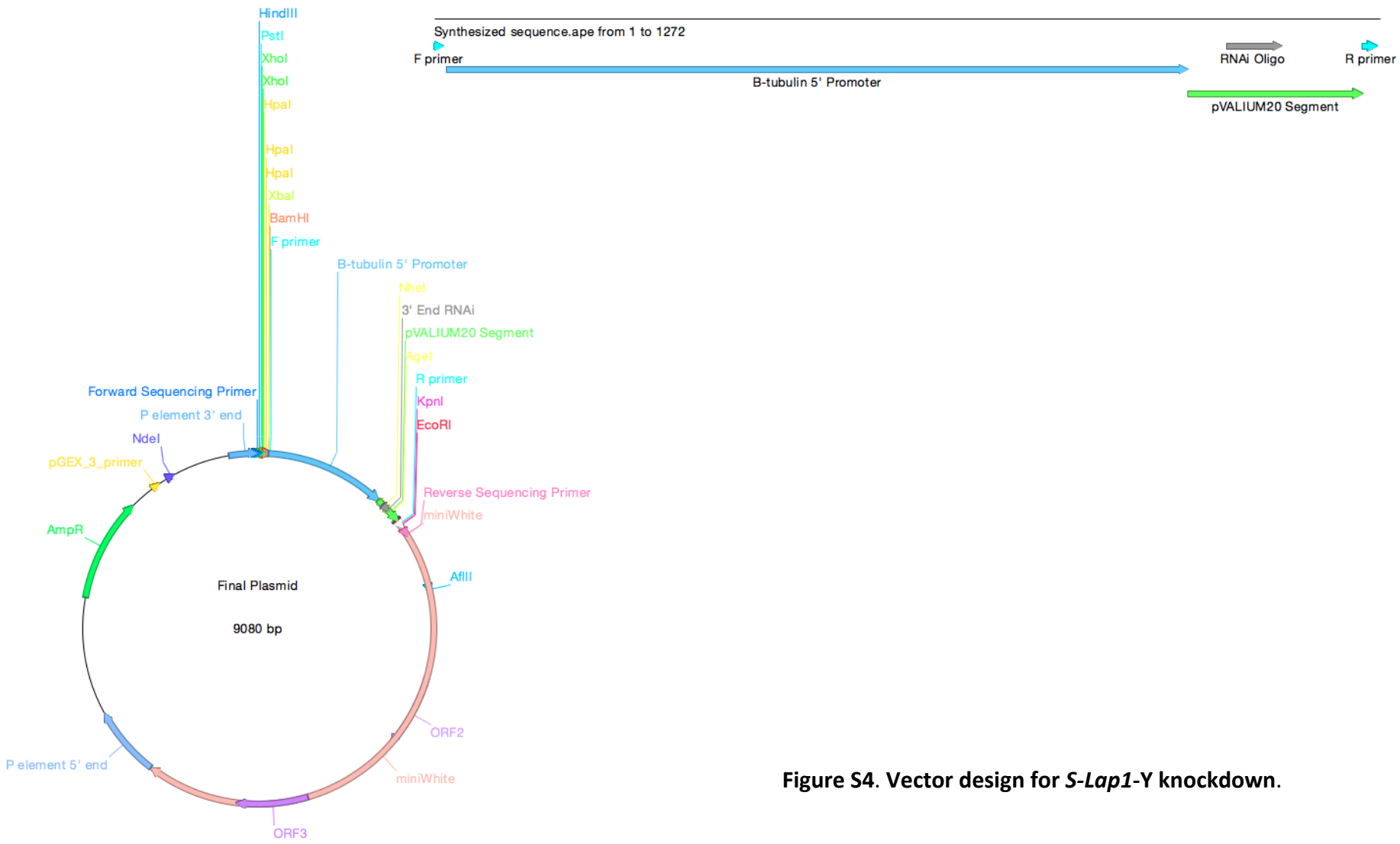

Figure S4. Vector design for *S-Lap1*-Y knockdown.

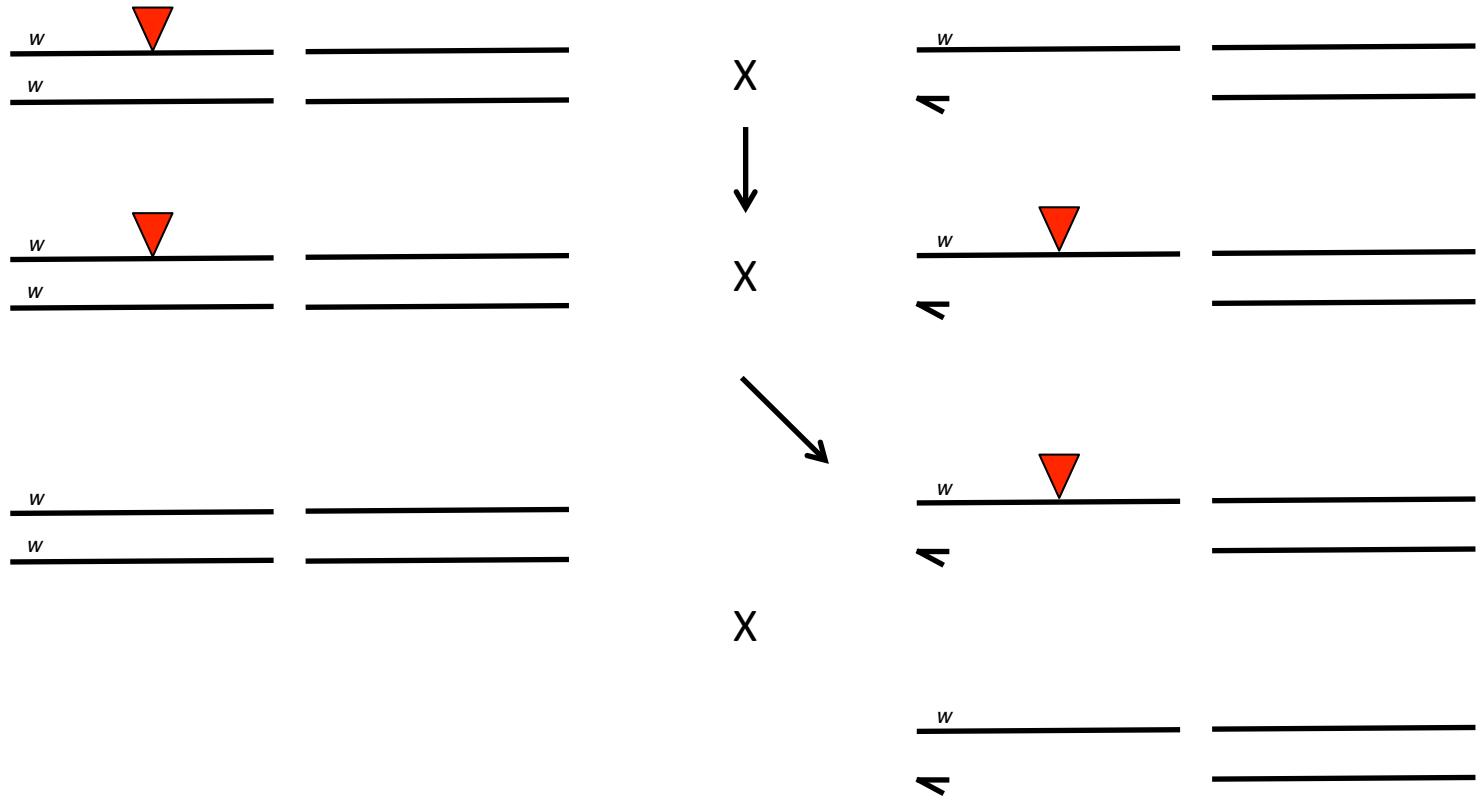

Figure S5. **Crossing design for assaying meiotic drive sex ratio.** Red-eyed *w; P(sh-S-LAP2)* virgin females were crossed to *w* males. The transgenes were determined to be X-linked based on progeny eye color. Red-eyed *w, P{sh-S-LAP2}* virgin female progeny were selected and crossed to *w, P{sh-S-LAP2}* progeny males. To assay sex ratio, 1-7 day old individual red-eyed *w; P(sh-S-LAP2)* males and 1-7 day old individual control *w* males were selected and crossed to five 1-7 day old virgin *w* females.

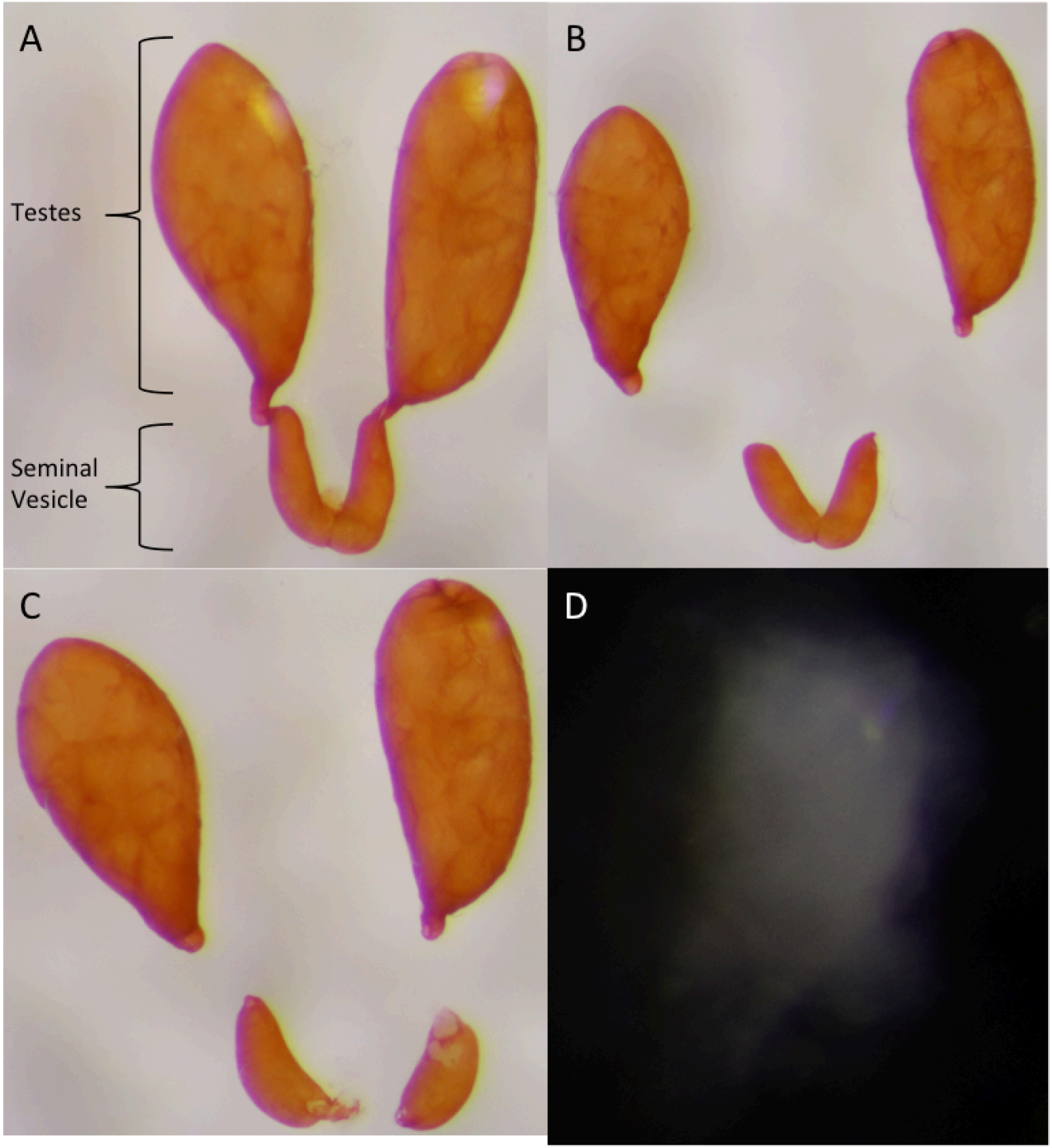

Figure S6. Testes and seminal vesicle dissections and sperm isolation. A. Testes and seminal vesicles were isolated, and connecting accessory glands were removed. **B.** Testes were isolated from seminal vesicles to be stored in Trizol for RNA extraction. **C.** Individual seminal vesicles were separated. **D.** Sperm was isolated from seminal vesicle by removing the encasing sheath, and stored in PBS for DNA extraction.

Table S1. Species used in this study. Shown are species and stock numbers, total assembly size, and sex chromosome karyotype (see Figure S1).

Data Generated for this Study					
Stock Center	**Stock Number**	**Genus**	**Species**	**Assembly**	**Karyotype**
UCSD	14045-0911.01	Drosophila	saltans	190 Mb	A + D
UCSD	15090-1692.12	Drosophila	nannoptera	135 Mb	A + D
UCSD	15040-1191.01	Drosophila	pseudotalamancana	146 Mb	A
UCSD	15250-2451.00	Drosophila	repletoides	166 Mb	A + D
UCSD	15020-1111.10	Drosophila	robusta	184 Mb	A + D
UCSD	15030-1151.01	Drosophila	micromelanica	146 Mb	A
UCSD	15030-1141.03	Drosophila	melanica	150 Mb	A + D
EHIME	E-22901	Drosophila	nigromelanica	164 Mb	A + C
EHIME	E-14007	Drosophila	lacertosa	155 Mb	A + D
UCSD	11010-0011.00	Scaptodrosophila	lebanonensis	215 Mb	A + F
UCSD	15172-2161.00	Drosophila	subbadia	174 Mb	A
UCSD	15172-2151.00	Drosophila	guarani	170 Mb	A
EHIME	E-14402	Drosophila	quadrilineata	166 Mb	A
UCSD	14024-0432.00	Drosophila	ercepeae	156 Mb	A
UCSD	92000-0075.00	Hirtodrosophila	duncani	205 Mb	A
UCSD	15210-2331.01	Drosophila	pallidipennis	167 Mb	A
UCSD	15010-1051.46	Drosophila	virilis	166 Mb	A
Published Data		**Genome Source**	**Male Illumina Reads**	**Female Illumina Reads**	
Drosophila	pseudoobscura	FlyBase	PMID: 25879221	PMID: 25879221	A + D
Drosophila	athabasca	PMID: 28431021	PMID: 28431021	PMID: 28431021	A + D
Drosophila	miranda	PMID: 22822149	PMID: 25879221	PMID: 25879221	A + D + C
Drosophila	albomicans	PMID: 22439699	PMID: 25879221	PMID: 25879221	A + D + C
Drosophila	novomexicana	This Study	PMID: 28739599	This Study: UCSD 15010-1031.00	A
Drosophila	americana	This Study	PMID: 28739599	This Study: UCSD 15010-1041.00	Male: A + B
Drosophila	lummei	This Study	PMID: 28739600	This Study: UCSD 15010-1011.09	A
Drosophila	busckii	PMID: 26114585	PMID: 25879221	PMID: 25879221	A + F
Drosophila	willistoni	FlyBase	This Study: 14030-0811.24	This Study: 14030-0811.24	A + D

Table S2. Multi-copy Y-linked genes in Drosophila species. Shown are the orthologous location of multi-copy Y genes in *D. melanogaster*, and their inferred molecular function and gene expression pattern in *D. melanogaster* (data from flybase.org).

Species	Chromosome	Peptide ID	Gene ID	InterPro Domain	Molecular Function	Testes_expression	Highest_Expression_Tissue	Highest_Expression_Development	Name	Gene Snapshot
albomicans_KM55	3L	FBpp0091021	FBgn0053725	Protein of unknown function DUF1091	NA	NA	NA	NA	NA	NA
americana	2L	FBpp0080666	FBgn0032715	Thiolase	transferase activity, transferring acyl groups other than amino-acyl groups	Y	Digestive System	Larva	NA	NA
athabasca_NJ28	2R	FBpp0071874	FBgn0045483	7TM chemoreceptor	taste receptor activity	NA	NA	NA	Gr59a	NA
athabasca_NJ28	2R	FBpp0085702	FBgn0034429	GNAT domain	N-acetyltransferase activity	N	Digestive System	Larva	NA	NA
athabasca_NJ28	2R	FBpp0085908	FBgn0034328	Immune-induced protein Dim	NA	N	Female Head	Adult Male	IM23	NA
athabasca_NJ28	3L	FBpp0088483	FBgn0036640	Leucine-rich repeat	May be involved in the export of mRNA from the nucleus to the cytoplasm	Y	Ovary	Embryo,Adult Female	nxf2	NA
athabasca_VAPW88	3L	FBpp0088483	FBgn0036640	Leucine-rich repeat	May be involved in the export of mRNA from the nucleus to the cytoplasm	Y	Ovary	Embryo,Adult Female	NA	NA
athabasca_VAPW88	3L	FBpp0310828	FBgn0266456	NA	NA	N	Salivary gland	Prepupae	NA	NA
lummei	X	FBpp0070717	FBgn0011761	Thioredoxin	female meiotic nuclear division, disulfide oxidoreductase activity	Y	Ovary	Embryo, Adult Female	dhd	Deadhead is a thioredoxin-like protein necessary for the initiation of embryonic development.
melanica	3L	FBpp0075822	FBgn0028668	V-ATPase proteolipid subunit	proton-transporting ATPase activity, rotational mechanism	Y	Testes	Adult Male	Vha16-2	NA
melanica	3L	FBpp0088546	FBgn0010424	EF-hand domain	calcium ion binding	Y	Carcass of larva	Embryo,Larva,Pupae	TpnC73F	NA
melanica	3L	FBpp0091046	FBgn0053796	Protein of unknown function DUF1091	NA	NA	NA	NA	NA	NA
miranda	2R	FBpp0071501	FBgn0026582	High mobility group box domain	nucleus	Y	Ovary	Embryo	Hmg-2	NA
miranda	2R	FBpp0072323	FBgn0060296	Ankyrin repeat	calcium channel activity, male courtship behavior	Y	Carcass of larva	Embryo,Larva,Pupae	pain	NA
miranda	3L	FBpp0072616	FBgn0004378	Kinesin motor domain; Kinesin-associated microtubule-binding domain	ATP-dependent microtubule motor activity	Y	Ovary	Embryo	Klp61F	Kinesin-like protein at 61F (Klp61F) is a member of the kinesin-5 family of cytoskeletal motor proteins. Klp61F allows the crosslinking and sliding apart of adjacent microtubules. This 'sliding filament mechanism' is critical for many aspect of mitosis and chromosome segregation.
miranda	2R	FBpp0085582	FBgn0034491	Hormone-sensitive lipase, N-terminal	lipase activity	Y	Ovary	Embryo	Hsl	Hormone-sensitive lipase is involved in lipid storage
miranda	2R	FBpp0085619	FBgn0005655	Proliferating cell nuclear antigen, PCNA	DNA binding, mitotic spindle organization	Y	Ovary	Embryo,Adult Female	PCNA	NA
miranda	2R	FBpp0085706	FBgn0034435	NA	spindle assembly involved in male meiosis I	Y	Testes,Imaginal Disc	Adult Male	fest	NA
miranda	2R	FBpp0085939	FBgn0034324	Protein of unknown function DUF1091	NA	NA	NA	NA	NA	NA
miranda	2R	FBpp0086004	FBgn0003701	NA	protein binding,mitotic sister chromatid segregation	Y	Ovary	Embryo	thr	Three rows (Thr) together with Sse forms the endoprotease separase complex, which cleaves a subunit of the cohesin complex, thereby allowing separation of the sister chromatids.
miranda	2R	FBpp0086750	FBgn0033860	Peptidase M17, leucine aminopeptidase/peptidase B	aminopeptidase activity	Y	Testes	Adult Male	S-Lap5	NA
miranda	2R	FBpp0086788	FBgn0033845	SAPAP family	microtubule binding,chromosome segregation	Y	Testes,Ovary	Embryo	mars	NA
miranda	2R	FBpp0086910	FBgn0033788	Transcription activator MBF2	NA	Y	Digestive System	Larva	NA	NA
miranda	2R	FBpp0087756	FBgn0033354	Fanconi anemia group I protein	DNA polymerase binding,mitotic G2 DNA damage checkpoint	Y	Ovary	Embryo	FANCI	NA
miranda	2R	FBpp0087986	FBgn0261385	Pleckstrin homology domain; Anillin homology domain	actin binding,male meiosis cytokinesis	Y	Ovary	Embryo	scra	Scraps is a homolog of anilin, a conserved pleckstrin homology domain (PLEKH) containing protein that binds actin, nonmuscle myosin II and microtubules. It stabilizes the contractile ring and is required for completion of cytokinesis

Table S2. - continued

miranda	2R	FBpp0088003	FBgn0033216	Diacylglycerol acyltransferase	transferase activity	Y	Digestive System	Embryo,Adult Male	NA	NA
miranda	X	FBpp0290242	FBgn0052666	Protein kinase domain	protein serine/threonine kinase activity	Y	Ovary, Salivary glad of prepupae	Embryo,Pupae,Adult Female	Drak	Death-associated protein kinase related (Drak) is a protein serine/threonine kinase belonging to the Death-associated protein kinase family. Drak promotes phosphorylation of sqh at sites known to stimulate actomyosin contractility. Its main characterized function is to shape epithelial tissues during development.
miranda	2R	FBpp0291585	FBgn0054045	NA	NA	NA	NA	NA	NA	NA
nannoptera	X	FBpp0077024	FBgn0031103	Protein of unknown function DUF4791	NA	Y	Testes	Adult Male	NA	NA
nigromelanica	2R	FBpp0085858	FBgn0063491	Glutathione S-transferase, N-terminal	glutathione transferase activity	Y	Head	Larva,Adult Male	GstE9	NA
nigromelanica	2R	FBpp0086954	FBgn0011604	ISWI family	DNA-dependent ATPase activity; nucleosome-dependent ATPase activity; protein binding; transcription factor binding; sperm chromatin condensation; spermatogenesis	Y	Ovary, Imaginal Disc and CNS of larva	Embryo	Iswi	NA
pseudoobscura_MV25	3L	FBpp0076362	FBgn0035915	Peptidase M17, leucine aminopeptidase/peptidase B	aminopeptidase activity	Y	Testes	Adult Male	S-Lap1	NA
pseudoobscura_MV25	3L	FBpp0076363	FBgn0052351	Peptidase M17, leucine aminopeptidase/peptidase B	aminopeptidase activity	Y	Testes	Adult Male	S-Lap2	NA
pseudoobscura_MV25	3L	FBpp0076372	FBgn0035916	Rab-GTPase-TBC domain	GTPase activator activity	Y	Ovary	Embryo	GAPsec	NA
pseudoobscura_MV25	3L	FBpp0112062	FBgn0035690	Zinc finger, AD-type; Zinc finger, RING/FYVE/PHD-type; Zinc finger C2H2-type	transcription factor activity, sequence-specific DNA binding	Y	Ovary	Embryo	NA	NA
robusta	3L	FBpp0072987	FBgn0010317	Cyclin-like	cyclin-dependent protein serine/threonine kinase regulator activity; mitotic cell cycle	Y	Ovary	Embryo, Adult Female	Cyclin J	NA
robusta	3L	FBpp0078102	FBgn0046301	Leucine-rich repeat domain	ubiquitin-protein transferase activity	Y	Testes	Embryo	NA	NA
robusta	3L	FBpp0312385	FBgn0053795	Protein of unknown function DUF1091	NA	NA	NA	NA	NA	NA

Table S3. **Down-regulation of Y-linked copies of S-Lap1 in P[w+;sh-SLAP] flies versus *white* control males.** To avoid cross-mapping of short RNA-seq reads between X and Y-derived transcripts, reads where only mapped to two regions with multiple fixed differences between the X and Y copies (Region_1 and Region_2; Region_2 corresponds to the genomic regions against which the hairpin RNA was designed). Both regions show about a 40% reduction in Y-linked transcripts in testis, compared to control *white* males.

	Y transcripts	
	Region_1: RPM (raw count)	Region_2: RPM (raw count)
P[w+;sh-SLAP] (Drive)	91.67 (1650)	142.56 (2566)
white Control	147.82 (3174)	238.12 (5133)
Drive/*w* Control	0.62	0.60
% reduction in drive	38%	40%

Table S4. **Embryonic hatch rates of transgenic P[w+;sh-SLAP] versus *white* control flies**. Differences in sex ratio between transgenic and control flies are not caused by male-specific embryonic lethality.

Embryonic hatch rates

Genotype	N[a]	Hatched	Unfertilized	Lethal	Total unhatched (unfertilitzed + lethal)
w	1933	1715 (88.7%)	137 (7.1%)	81 (4.2%)	218 (11.3%)
P[w+:sh-SLAP2]2	1743	1524 (87.4%)	148 (8.5%)	71 (4.1%)	219 (12.6%)
P-value[b]		0.73	0.68	0.72	0.69

[a] Number of individual embryos assayed for hatching
[b] two-sample t-test